International Journal of Modern Manufacturing Technologies
ISSN 2067–3604, Vol. XI, No. 1 / 2019

PROPERTIES ANALYSIS OF HOMOGENEOUS WELDING JOINTS OF THE DUPLEX – AUSTENITIC STEEL TYPE WELDED WITH AUSTENITIC WIRE

Santina Topolska [1], Aleksander Gwiazda[2]

[1] Silesian University of Technology, Faculty of Mechanical Engineering, Institute of Engineering Materials and Biomaterials, Konarskiego 18A, 44-100 Gliwice, Poland
[2] Silesian University of Technology, Faculty of Mechanical Engineering, Institute of Engineering Processes Automation and Integrated Manufacturing Systems, Konarskiego 18A, 44-100 Gliwice, Poland

Corresponding author: Santina Topolska, santina.topolska@polsl.pl

Abstract: The article presents the structure and properties of dissimilar welded joints based on duplex 2205 and austenitic 316L stainless steels manufactured using Avesta P5 austenitic binder. The purpose of researches was to analyze the impact of joint type and binder material on the mechanical properties of these welded joints. Hardness measurements were carried out in accordance with PN-EN ISO 9015-1: 2011. The tests were carried out using the Vickers method, with a load of 49.03 N (HV5). It was shown that the hardness of welds is intermediate between the hardness of base materials, where hardness in the HAZ (Heat Affected Zone) area is higher on the 2205steel side.

Key words: Duplex steel 2205, austenitic steel 316L, welded dissimilar joints, hardness

1. INTRODUCTION

Duplex steel is a type of steel with a two-phase structure in which each phase occurs in a significant volume (within 50%). Most often this term refers to the ferritic-austenitic steel, although there is steel with the martensitic-ferritic structure, which was used at the beginning of the 20th century. In this paper, the term “duplex steel” refers only to the first group of steels, i.e. austenitic-ferritic steels, in which the ferrite content varies from 30 to 70%.

Duplex steel combines the advantages of both austenitic steel and ferritic steel. Ferrite provides the steel with the required strength and resistance to stress corrosion, while austenite provides the appropriate plastic properties [1]. Currently, the 4th generation of duplex steels is being implemented [2]. The first generation of these steels contained approx. 18% Cr, (4-6)% Ni and sporadically Mo. Sometimes, however, there were problems with their weldability. In addition, large amounts of ferrite were formed in the welded joints, which greatly reduced the corrosion resistance and toughness of these steels.

Currently, due to the modification of the chemical composition and production technology, problems with their weldability have been significantly reduced [3,4].

The average content of alloying elements in duplex steels is nowadays: around 0.03% C, (21-29)% Cr, (2.5-8)% Ni, up to 5% Mo, up to 0.36% N, up to 2.5% Cu, and 1.0 to 5.4% Mn. It should be emphasized that the chemical composition of the duplex steel is selected so as to ensure good pitting corrosion resistance and good stress corrosion resistance.

2. RESEARCH METHODOLOGY

2.1. Types of dissimilar joints

For the research, the butt joint was selected as the one which is characterized by a more complex state of stress and allows for more direct assessment of phenomena affecting the properties of the entire welded joint. Four types of butt joints were selected for research purposes as technical variables of the analyzed process [5]. The selected butt joints were:

-square groove weld (I), made without chamfering edges with a gap of 1 mm, double-sided, two-pass welded (No 1);

-single-Vee butt weld (Y) with groove face chamfered at 30^o (groove angle of 60^o opening, groove depth 11mm, root face thickness 4 mm, opening 1mm), single-sided, multi-pass welded, limited heat impact (No 2A);

-single-Vee butt weld (Y) with groove face chamfered at 30^o (groove angle of 60^o opening, groove depth 11mm, root face thickness 4mm, opening 1mm), single-sided, multi-pass welded (No 2B);

-double-Vee butt weld (2Y) with 45° bevel angle (groove angle of 90°, 5.5mm groove depth, 4mm root face thickness, 1mm root opening), double-sided, two-pass welded (No 3).

Joints No 2A and No 2B differ in the number of passes and heat inputs value. The first joint was welded with heat input limited to 1.5kJ/mm. In the case of the joint No 2A the number of passes was equal to 9 and in the case of the joint No 2B to 5.

The method of edges preparation for welding for the indicated butt joints is shown below (Figure 1). The chamfering was done with milling. Before welding, the chamfered edges were sanded to clean the surface.

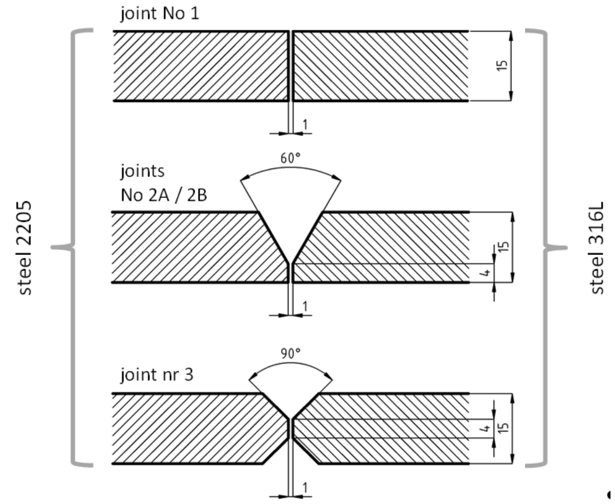

Fig. 1. Edge preparation for analyzed welded joints, [own elaboration]

Welded joints were made using the 3,2 mm AVESTA P5 welding wire with austenitic structure with 5 - 10% of ferrite (designation according to EN ISO 14343: S 23 12 2 L, designation according to AWS A5.9: ER309LMo). This wire is characterized by the ferrite number 8 (deLong) or 9 (WRC-92) [15]. The highest value of the heat input, during welding, was equal to 3.64kJ/mm (joint No 2B) and the lowest value was equal to 1.19 kJ/mm (joint No 2A).
Welding was made with a submerged arc (SAW) in the low position, which was selected due to the fact that in the smallest way affects the characteristics of the obtained welded joints. The electrode in the welding machine was set horizontally. All detailed welding process parameters for the indicated four types of joints are presented in Table 1.

Table 1. Welding parameters, [5]

Joints No	Flux	Weld type	No of passes	Heat input [kJ/mm]	Pass
1	AVESTA P5 AVESTA P5	I	2	2.66 2.66	1/1 2/1
2A	BOEHLER CN 23/12 Mo BOEHLER CN 23/12 Mo AVESTA P5 AVESTA P5 AVESTA P5 AVESTA P5 AVESTA P5 AVESTA P5 AVESTA P5	Y	9	1.19 1.19 1.16 1.16 1.16 1.16 1.16 1.44 1.44	1/1 1/2 1/3 1/4 1/5 1/6 1/7 1/8 1/9
2B	BOEHLER CN 23/12 Mo AVESTA P5 AVESTA P5 AVESTA P5 AVESTA P5	Y	5	1.22 1.26 1.38 3.64 2.91	1/1 1/2 1/3 1/4 1/5
3	AVESTA P5 AVESTA P5	2Y	2	2.23 3.28	1/1 2/1

Since all welds were manufactured in more than one-pass, the important, in the case of the duplex steel welding, was the height of the inter-pass temperature. It was assumed that it will not exceed 100°C. The measurement was made with a photoelectric pyrometer. In the case of joints No 2A and No 2B, the BOEHLER CN 23/12 Mo flux was used for making the penetration passes.

3. RESULTS

3.1 Metallographic examinations

Specimens for microscopic observations were prepared using the Marble reagent ($CuSO_4$, HCl). The metallographic microsections were etched with this reagent to reveal the characteristic elements of the welded joint cross-section (fusion lines, heat affected boundaries). They allow finding content of austenite and ferrite, the presence of secondary austenite and precipitations of any intermetallic phases. Generally, these observations allowed concluding that austenite mainly is in the form of dendrites in the cross-section of the weld. Ferrite occurs in the form of precipitates located between austenite dendrites. The proportion of ferrite, based on image analysis, should be assessed as being in the range of (10-20)%. Figure 3 presents this type of phase system. A higher proportion of ferrite should be noted only in the area of the weld at the border with the steel 2205. It is the result of ferrite penetration from the area of two-phase steel. The HAZ (Heat Affected Zone) areas were subjected to more detailed observations. Generally, it should be stated that their width is rather small, however on the 2205 steel side HAZ is clearly wider than on the side of the 316L steel. On the 2205 steel side, the HAZ width varies between 300 and 600μm. However, on the side of steel 316L its width varies between 100 and 300μm. Thus, it can be concluded that the HAZ on the 2205 steel side is 2 to 3 times greater than on the 316L steel side.
In the metallographic view of the weld No 1, attention should be paid to the fairly homogeneous structure of the weld material due to the high degree of penetration of the welded material (Figure 2). Moreover, a slightly larger HAZ width is observed than in multi-pass welds, especially in the middle area, which is shown in Figure 3. However, the structure of the HAZ itself is more ordered. Attention should also be paid to the phase system in HAZ 2205, which is poorly ordered due to the influence of welding energy. However, due to the small number of passes (thermal cycles), the number of dendrites occurring in this area is also rather low and they do not change the characteristics of the joint.
In the case of joint No 2A, the structure of the weld area should be assessed as even less ordered (Figure 2). Dendrites in the weld area are not so densely packed.

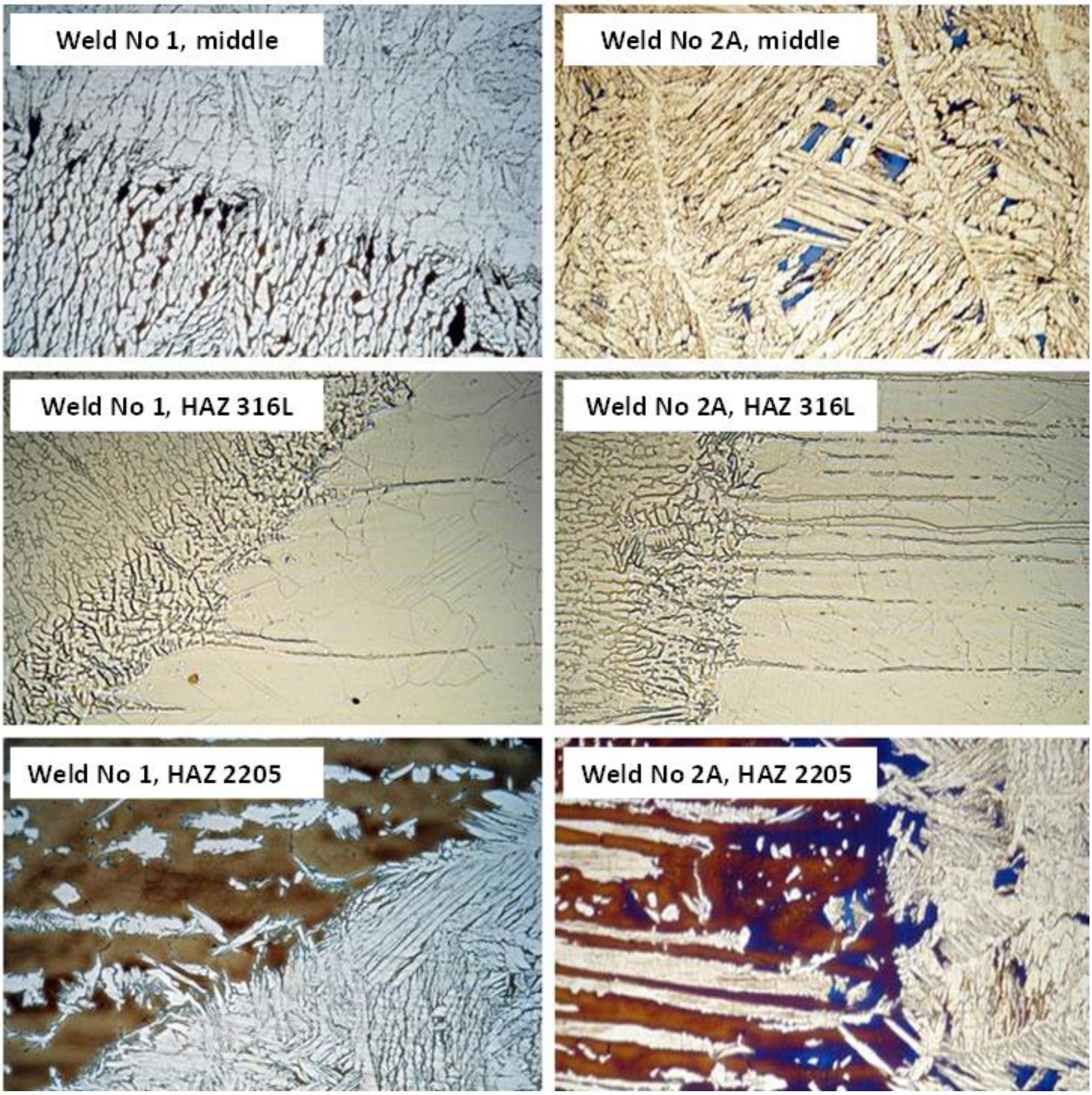

Fig. 2. Comparison of metallographic images of joints No 1 and No 2A

In the area of HAZ 316L of the joint No 2A, the rather irregular course of the thermal interaction boundary can be observed. This is due to the multiplicity of thermal cycles that modified its course. On the other hand, the area of HAZ 2205 is characterized by maintaining a linear arrangement of austenite grains, which results from the low linear energy of welding.

Conclusions, similar in nature, can also be formulated as generalizations of the metallographic study of the joint No 2B (Y-joint, multi-pass). The structure of the weld area resembles that of the microscope image of joint No 1 (Figure 3). It is quite homogeneous, and the grains are rather small in size. The HAZ 316L structure is unordered. The dendrites of the HAZ 2205 area are large, and their distribution in this zone is quite rare.

Finally, the last weld that should be analyzed is the joint No 3 (2Y, two-side weld). Dendrites in the weld area of this joint are of medium size and moderately ordered as shown in Figure 3. The area of HAZ 316L is the same width as in the case of the joint No 1, but relatively less ordered.

In contrast, the HAZ 2205 zone is characterized by a greater number of ordered dendrites, which is somewhat reminiscent of the structure of this area in the previously analyzed joint No 2A. Therefore, taking into account the metallographic images of the studied joints, the joint No 2A and the joint No 3 should be indicated as the best ones from the structural point of view.

The conducted metallographic examinations allow analyzing the later results relating to mechanical characteristics investigation.

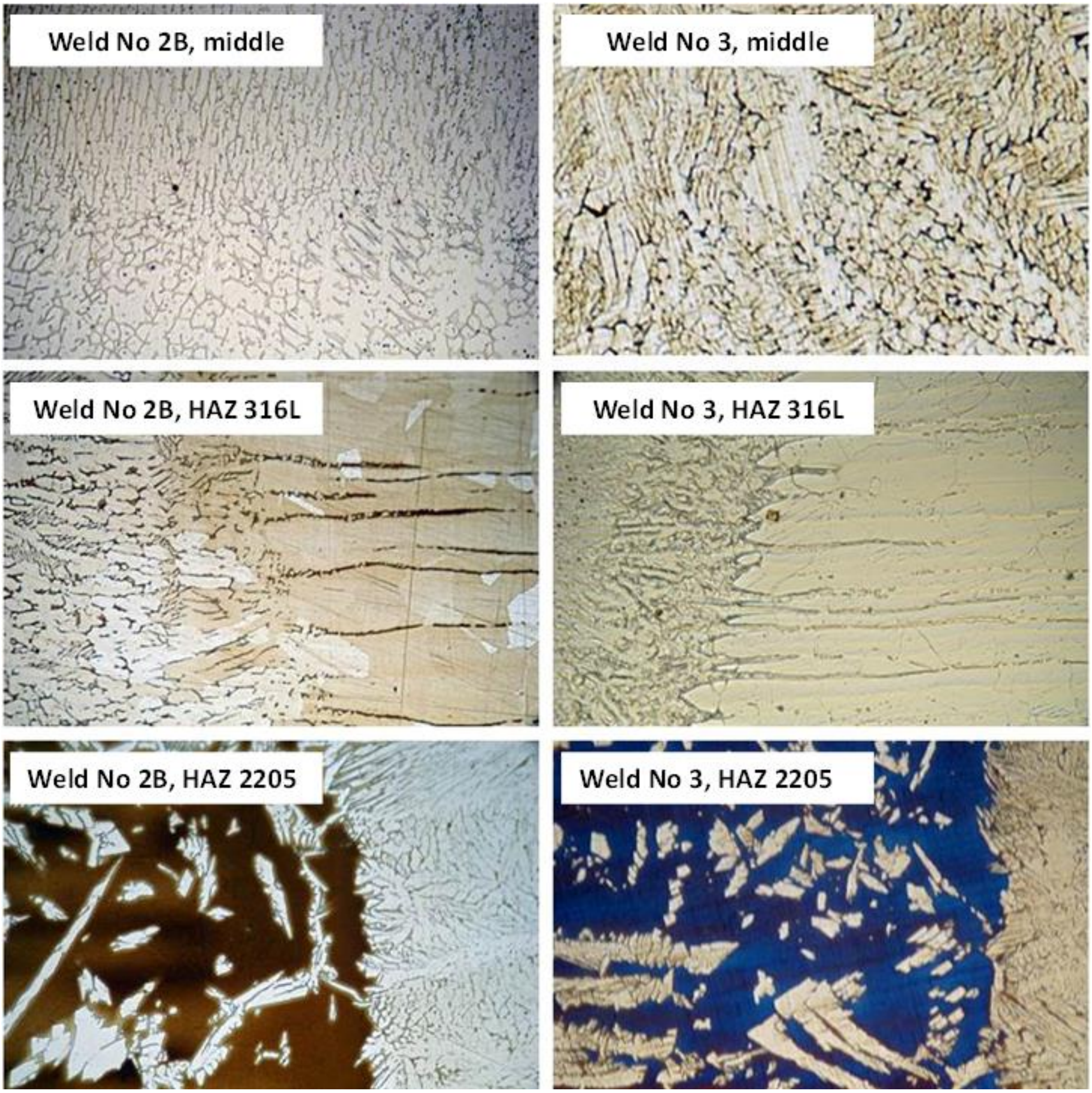

Fig. 3. Comparison of metallographic images of joints No 2B and No 3

3.1 Hardness examinations

Hardness was measured on samples taken for metallographic researches described previously. They contained the central element of the welded joint and were cut perpendicular to the axis of the weld. In relation to these cross-sectional elements, hardness measurements were carried out. Three transversal hardness measurement lines were designated on the weld cross-sections. The first one was lying near the face of the weld, the second was in the middle of the specimen and the third measuring line was determined near the root of the weld. In Figure 4 the results of hardness tests, for all analyzed in the paper types of welded joints, are presented. In this Figure are indicated average hardness values for points lying in the same position measured in the mentioned three measuring lines.

When assessing the value of the determined average hardness values, it should be noted that the highest ones characterize the joint No 2A. In the second place is the joint No 1 before the joint No 3. Similar in the characteristics is the structure of hardness observed on the horizontal cross-section of analyzed joints

Analysis of average hardness values in the areas of HAZ 2205 and HAZ 316L as well as the distribution of average hardness values in the weld axis, shows that the most varied is the characteristics of average hardness values in the axis of the weld. Taking into account the results, presented in Figure 7, it can be considered that the best in this respect are: the joint No 2A and the joint No 3. It is related from low heat input (joint No 2A) and low number of thermal cycles (joint No 3).

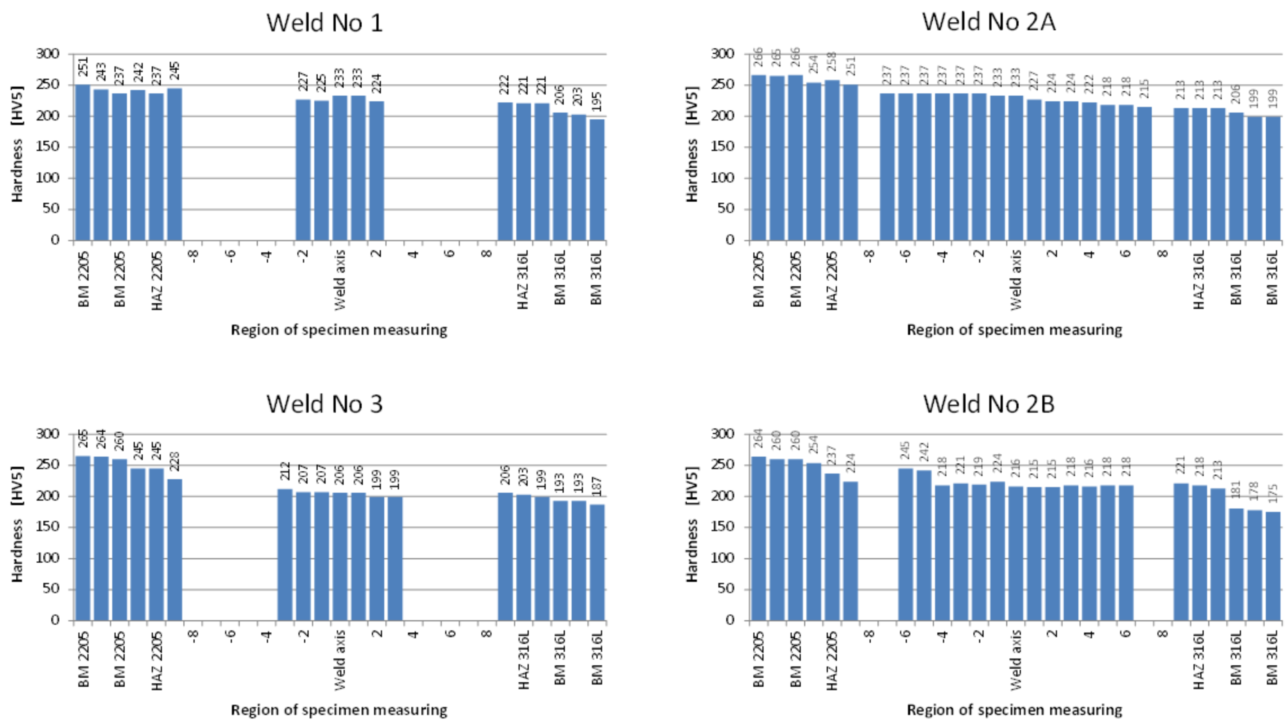

Fig. 4. Results of hardness tests

3.2. FEM analysis

To conduct analysis without preparing additional specimens special virtual model of the joint was prepared (Figure 5). Its characteristics were based on the material tests. The model was subjected to the virtual tensile tests (Figure 6).

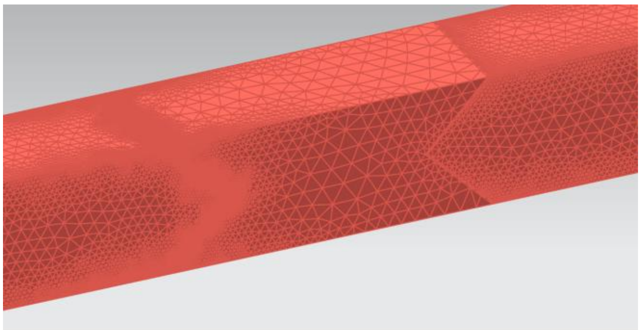

Fig. 5. Elaborated joint model

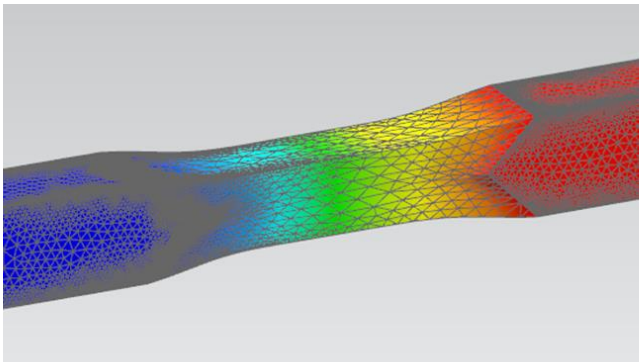

Fig. 6. Stretching test

Particular emphasis was placed on modeling the HAZ zones. In the Figure 7 is presented the stress distribution in the HAZ 2205 zone (inside the specimen) and in the Figure 8 is presented the stress distribution around the HAZ 316L area. Places of the stress increase are clearly visible.

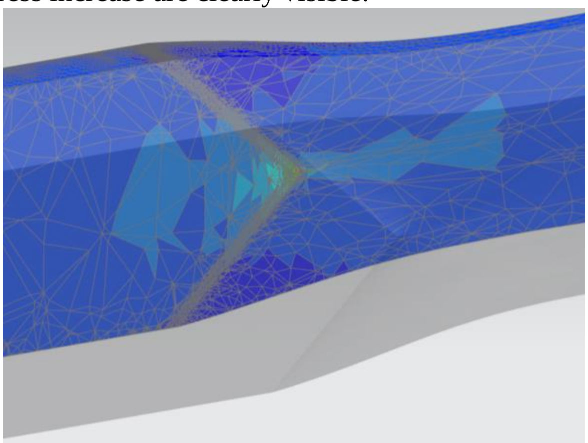

Fig. 7. Stresses around HAZ 2205

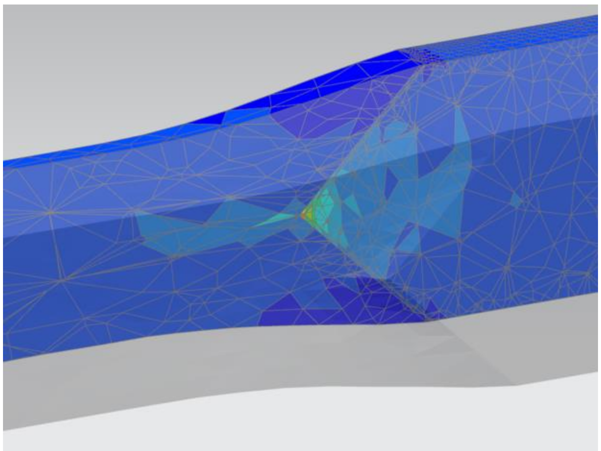

Fig. 8. Stresses around HAZ 316L

The proposed FEM approaches are resulted from the analysis of similar approaches in other scientific investigations [6-8]. In the presented approach however the material characteristics and the structure of the joint are based on the previous metallographic analysis of the real one. To verify the results of the virtual model test it was conducted a series of tensile test of the real specimens of the joints. According analysis it was shown that the concentration of stresses is observed in the area of the 316L base material. During tests the fracture also was observed in this area (Figure 9).

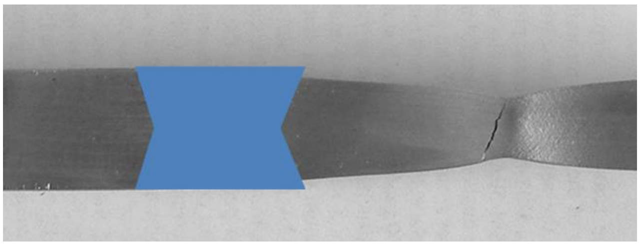

Fig. 9. Exemplar results of tensile test

In the Figure above it was marked (blue) the area of the weld, hence it is not visible on the photograph.

4. CONCLUSIONS

Analyzing the results, it should be stated that the highest average hardness (HV5) is characteristic for the joint No 2A, and the lowest value for the joint No 2B (difference of 8%). This confirms the relationship between the linear welding energy (heat input) and the grain size of the main phases (2A fine grained, and 2B coarse grained). In the cross-section of the investigated joints, the highest values were measured on the side of HAZ 2205 (HV5 on average 243), and the lowest on the HAZ 316L side (HV5 on average 210). In the axis of the weld the root proved to be the hardest (HV5 average 236), and the least hard area was the face (HV5 average 215).

The similar results have been obtained using the FEM model described in the paper. It allows developing the works leading to elaborate the FEM-based method to predict the mechanical properties of such type of welded joints. The next work will be related with more specific approach to the weld structure modeling, including HAZ'es as well as more specific defining the material properties to better model the behavior of the real joint.

5. REFERENCES

1. Nowacki, J., (2009). *Duplex steel and its weldability*. Wydawnictwa Naukowo - Techniczne, Warszawa (in Polish).
2. Gunn, R. N., (2003). *Duplex Stainless Steels: Microstructure, Properties and Applications*. Abington Publishing, Cambridge.
3. Lippold, J. C., (2015). *Welding Metallurgy and Weldability*. John Wiley and Sons, Hoboken.
4. Davies, A. C., (2003). *The Science and Practice of Welding*. Vol. 2, Cambridge University Press, Cambridge.
5. Topolska, S., (2017). *Properties and morphology of dissimilar welding joints of a duplex steel and an austenitic one*. Wydawnictwo Pracowni Komputerowej Jacka Skalmierskiego, Bytom (in Polish).
6. Szávai, S., Bezi, Z., Ohms, C., (2016). *Numerical simulation of dissimilar metal welding and its verification for determination of residual stresses*. Fratt. Integr. Strutt., 36/10, 36-45.
7. Del Coz Díaz, J. J., Menéndez Rodríguez, P., García Nieto, P. J., Castro-Fresno, D., (2010). *Comparative analysis of TIG welding distortions between Austenitic and Duplex Stainless Steels by FEM*. Applied Thermal Engineering, 30(16), 2448-2459.
8. Koňár, R., Patek, M., (2017). *Numerical Simulation of Dissimilar Weld Joint in Sysweld Simulation Software*. Tehn. Vj., 24(1), 137-142.

Received: November 13, 2018 / Accepted: June 15, 2019 / Paper available online: June 20, 2019